Asian Journal of Chemistry; Vol. 38, No. 1 (2026), 223-233
ASIAN JOURNAL OF CHEMISTRY
https://doi.org/10.14233/ajchem.2026.34948

Adsorption of Ammonium Ions from Water using Activated Carbon Derived from Garlic Waste

N.D. SHOOTO*, and P.M. THABEDE

Water Treatment Laboratories, Department of Natural Sciences, Vaal University of Technology, Private Bag X021, Vanderbijlpark 1900, South Africa

*Corresponding author: E-mail: ntaotes@vut.ac.za

Received: 24 September 2025 *Accepted*: 16 December 2025 *Published online*: 31 December 2025 AJC-22242

Water contaminated with ammonium (NH_4^+) is associated with many adverse effects on humans, aquatic organisms and the environment. The removal of NH_4^+ from aquatic sources is essential to support life. This study used modified garlic basal plate waste to remove NH_4^+ from polluted water. Garlic waste was carbonized at 450 ºC and chemically activated with NaOH and H_3PO_4. After activation, the samples were characterized using SEM, EDX, TEM, XRD, FTIR and Raman spectroscopy. The SEM images showed that the inner surface was exposed and was heterogeneous and, porous with cavities of different sizes and shapes. The elemental constituents of the materials are carbon (C), oxygen (O) and heteroatoms in trace amounts. FTIR analysis showed that the materials have many functional groups, such as –OH (3250 cm^{-1}), –CH (2916 cm^{-1}), –C=C and –NH_2 groups (1658 cm^{-1}), –OH (1425 cm^{-1}) and –CO (1000 cm^{-1}). Equilibrium studies indicated that the data fit the nonlinear Freundlich model, suggesting that the uptake represents multilayer adsorption due to different active sites on the adsorbent with unequal energy levels. The Freundlich constant (*n*) values were between 4.276 and 5.902, indicating that the uptake was favourable. The contact time effect showed three different phases of adsorption: a strong uptake, a steady state of adsorption and a plateau. The data for the contact time corresponded to the pseudo-second order kinetic model. The ΔH^o values ranged from (-1.27 to -5.04 KJ/mol), indicating that the uptake was dominated by physical adsorption, but to some extent other mechanisms were partially involved in the uptake. The values of ΔS^o and ΔG^o were also negative, indicating that the adsorption was spontaneous and only partially random. The optimal conditions for the uptake of NH_4^+ using a working standard with an initial concentration of 100 mg/L were a solution pH of 10 and a temperature of 298 K. Under these conditions, the adsorption capacities for untreated carbon from garlic basal plate (CGBP), acid activated garlic basal plate (AGBP) and base activated garlic basal plate (BGBP) were 25.09, 37.04 and 40.11 mg/g, respectively.

Keywords: Garlic basal plate waste, Activated carbon, Adsorbents, Ammonium ions.

INTRODUCTION

Ammonium (NH_4^+) is formed when ammonia gas dissolves in water. NH_4^+ enters the environment and aquatic systems from fertiliser manufacturers, paper mills and textile and rubber factories [1,2]. Other sources include agricultural and domestic wastewater containing household cleaners that enter the municipal sewage system [3]. Water pollution by ammonium (NH_4^+) is widespread throughout the world.

Water polluted with excess NH_4^+ is associated with negative effects such as eutrophication, water discolouration due to algal blooms, bacterial overgrowth and increasing acidification making it harmful to aquatic organisms, humans and the environment [4]. The acceptable level of NH_4^+ in surface waters is up to 12 mg/L [5]. Exceeding this limit damages the gills of some aquatic organisms, leading to respiratory problems and eventually death [6]. Excess NH_4^+ also damages several internal organ systems in humans [7,8].

The removal of excessive NH_4^+ from water is necessary for the survival of all living organisms. Among the many methods used to remove pollutants from water, adsorption is favoured because it is versatile, effective, inexpensive, easy to carry out and eco-friendly too [9]. Different types of materials such as activated carbon, agricultural waste, clay, natural and synthetic materials, *etc*. can be used as adsorbents [10,11].

Agricultural waste that is normally discarded can be used as an adsorbent due to its low cost and easy availability [12]. Plant-based agricultural wastes consist of cellulose, hemicellulose and lignin. The lignocellulosic materials provide functional groups that can bind pollutants [13]. The main limi-

tations of plant-based materials as adsorbents include low surface area, poor cation exchange capacity and difficulty in removing the adsorbed materials [14]. This limits the use of these materials in water treatment. However, carbonization and activation significantly improve the physical and chemical properties of agriculture waste [15].

Garlic is grown in many parts of the world because of its health benefits and nutrient content [16]. It is a natural antibiotic and antifungal agent. Garlic is one of the most widely used herbs in the world and is used in households, restaurants and the food industry to produce spices. Garlic bulbs are composed of cloves and the non-edible parts, including skins (peels) and base plates, are discarded as waste, which can be harmful to the environment.

Activated carbon is widely used for water treatment due to its porous structure, oxygen-containing functional groups, and high surface area [17], but its major limitation is the high production cost [18,19]. Low cost, plant-based materials such as garlic peels have been studied extensively for water treatment, for various pollutants such as the metal ions Pb(II), Cu(II) and Ni(II) [20], Cd(II) [21], Cr(VI) [22], Tb(III) [23]; organic substances and dyes such as phenol [24], methylene blue [25,26], malachite green [27] and rhodamine B [28]; pharmaceutical products such as enrofloxacin [29]. The great potential of using garlic peels as adsorbents in water purification, provides a good basis for using other parts of garlic.

This may be the first report of converting garlic basal plate waste into a valuable material and simultaneously reducing the solid waste in the environment. The waste was carbonized at 450 ºC to obtain carbon from garlic basal plates (CGBP). This material, was chemically activated with 5 M acid (H_3PO_4) and base (NaOH) and labelled as AGBP and BGBP, respectively. No reported study has used carbon from garlic basal plate as a potential adsorbent for NH_4^+. In this work, the effects of initial concentration, contract time, solution pH, reaction temperature, reusability and regeneration studies were investigated.

EXPERIMENTAL

Garlic waste was obtained from a local vegetable shop in Vanderbijlpark, South Africa. Ammonium chloride ≥ 99.5%, hydrochloric acid ≥ 37.0%, sodium hydroxide ≥ 98.0% and phosphoric acid ≥ 25.0% were purchased from Sigma- Aldrich (Johannesburg, South Africa).

Carbonized garlic basal plate: The garlic basal plate was ground to powder using a pulveriser. Exactly 10 g of ground material was transferred and carbonized in a furnace at 450 ºC under nitrogen flow. After 30 min the sample was collected and designated carbon from garlic basal plate (CGBP).

Activated carbon: Exactly 5 g of CGBP was added to 400 mL of 5 M NaOH in a 500 mL beaker and agitated at 350 rpm for 60 min, after which the sample was rinsed four times with distilled water to remove excess NaOH, oven-dried at 45 °C for 5 h, and labelled as base-activated garlic basal plate (BGBP).The same procedure described above was followed for the preparation of acid-activated garlic basal plate (AGBP) using 5 M phosphoric acid.

Preparation of stock solution and working standards: A solution of NH_4Cl (100 mg/L) was prepared by dissolving the salt in 1 L distilled water in a volumetric flask. This solution was diluted for the preparation of 80, 60, 40 and 20 mg/L solutions in 200 mL volumetric flasks.

Adsorption methodology: The adsorption experiments were carried out by using 100 mg of sorbent material in 50 mL solution containing NH_4^+ ions agitated at 200 rpm for 240 min unless otherwise stated. The effect of pH was examined between pH 2, 4, 6, 8 and 10 on standardized solution 100 mg/L at 283 K. The effect of contact time was carried out between 5-240 min on a standardized solution of 100 mg/L at 283, 293 and 303 K agitated for 240 min. The initial concentration and temperature effects were analysed on standard solutions of 20, 40, 60, 80 and 100 mg/L at 283, 293 and 303 K agitated for 240 min. The experiments were carried out in triplicate to ensure repeatability.

Sorption data management: The removal, q_e (mg/g) of NH_4^+ by CGBP, AGBP and BGBP was calculated using eqn. 1.

$$q_e = \frac{(C_o - C_e)V}{W} \quad (1)$$

Initial and equilibrium concentrations are represented by C_o and C_e; the volume is V and the adsorbent mass is W.

Adsorption kinetics were evaluated using non-linear models of pseudo-first-order (PFO) and pseudo-second-order (PSO) in eqns. 2 and 3, respectively.

$$q_e = q_t(1 - e^{-k_1 t}) \quad (2)$$

$$q_e = \frac{1 + k_2 q_e t}{k_2 q_e^2 t} \quad (3)$$

where q_e (mg/g) and q_t (mg/g) stand for the uptake of pollutants at equilibrium and time, t (min), respectively. K_1 (min^{-1}) is the PFO rate constant, and k_2 (g mg/min) is the PSO rate constant.

Non-linear adsorption isotherms Langmuir and Freundlich were calculated using eqns. 4 and 5, respectively:

$$q_e = \frac{Q_o b C_e}{1 + bC_e} \quad (4)$$

$$q_m = k_f C_e^{1/n} \quad (5)$$

where, Q_o (mg/g) is designated for the adsorbed pollutant, symbol b represents the constant of Langmuir interaction energy. q_m (mg/g) stands for the adsorption capacity, k_f and $^1/_n$ are Freundlich's capacity factor and constant. The non-linear model parameters were determined using origin 2015.

Non-linear adsorption isotherm models were validated using Marquart's percentage standard deviation (MPSD) shown in eqn. 6:

$$MPSD = 100\sqrt{\frac{1}{N-p}\sum_{i=1}^{N}\left(\frac{q_{e,exp} - q_{e,cal}}{q_{e,exp}}\right)^2} \quad (6)$$

The thermodynamic parameters enthalpy change ΔH^o (KJ/mol), entropy change ΔS^o (KJ/mol), and standard free energy change ΔG^o (KJ/mol) were determined at various ambient temperatures (288, 298 and 308 K) using eqns. 7 and 8:

$$\ln K_c = -\frac{\Delta H^o}{RT} - \frac{\Delta S^o}{R} \quad (7)$$

$$\Delta G^{o} = -RT \ln K_c \quad (8)$$

where K_c stands for Langmuir equilibrium constant. ΔH^{o} and ΔS^{o} were calculated from the graph of $\Delta G^{o}/RT$ *versus* 1/T as slope (gradient) and intercept respectively. While, R stands for the gas constant (8.314 K/mol) and T (K) is designated to the temperature.

Characterization: SEM coupled with EDX (Thermo-Fisher, Waltham, MA) was used to characterise the surface morphology and the elemental constituents of the adsorbents. XRD (Shimadzu Corporation, Kyoto, Japan) was used to analyse the purity of the adsorbents. FTIR (Perkin-Elmer, Waltham, MA, USA) was used to identify the moieties on the surface of the adsorbents. Raman spectroscopy (Jobin-Y von T64000, Horiba Scientific, Northampton, U.K.) was used to investigate the adsorbents graphitic structure. TEM (Joel Ltd., Tokyo, Japan) was used to study the morphology of the adsorbents. A UV-visible spectrometer (Thermo-Fisher Scientific) was used to confirm the concentration of NH_4^+ in the solution before and after adsorption.

RESULTS AND DISCUSSION

SEM analysis: The SEM images of the surface and morphology of the samples are shown in Fig. 1a-f. The CGBP (Fig. 1a-b) sample showed that the morphology of the untreated carbon is amorphous with an irregular surface (Fig. 1b). After chemical treatment, the inner surfaces of AGBP and BGBP were exposed. The surface is heterogeneous and porous with voids of different shapes and sizes. These characteristics are typical for activated carbon materials [30]. The pores and voids on the surface of the adsorbents are important features that significantly enhance adsorption processes, primarily through increased surface area, enhanced interactions and pollutant entrapment within the pores [31]. Moreover, treatment of carbon with H_3PO_4 and NaOH modifies the functional groups on the adsorbent by introducing groups such as hydroxyl and carboxyl [32].

TEM studies: The TEM images (Fig. 2a–c) were further analyzed to reveal the morphological features of the samples, showing varying light and dark grey regions, where the darker areas are attributed to overlapping particles and confirming an amorphous morphology typical of carbon-based materials.

EDX analysis: The elemental analysis of the materials was determined using EDX (Fig. 3a-c). The main elemental constituents of CGBP are carbon (C) and oxygen (O). The other elements are traces of heteroatoms which occur naturally in the garlic basal plate. Some heteroatoms were cleaved after chemical activation. In AGBP, the content of phosp-

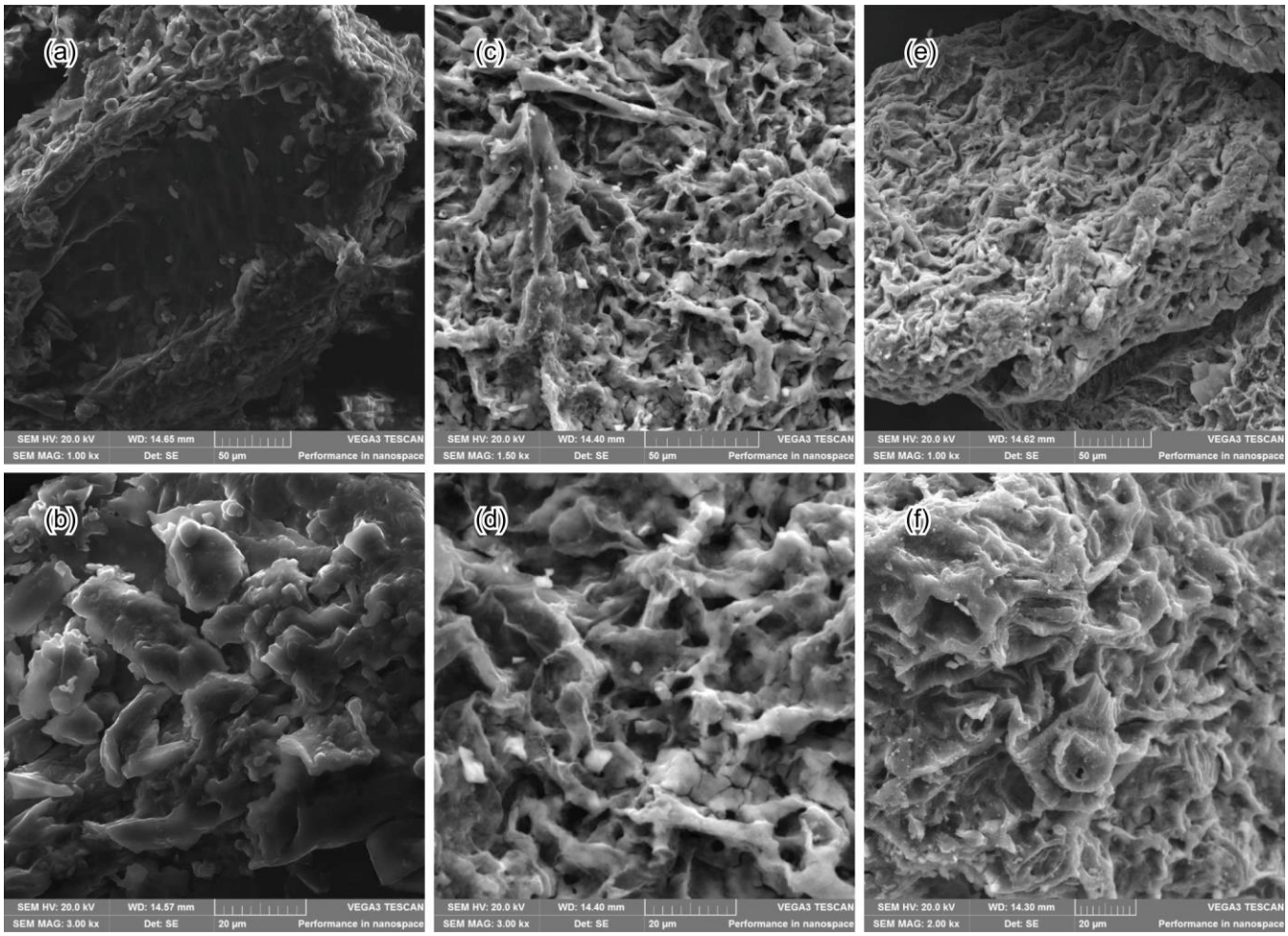

Fig. 1. SEM images of (a-b) CGBP, (c-d) AGBP, (e-f) BGBP adsorbents

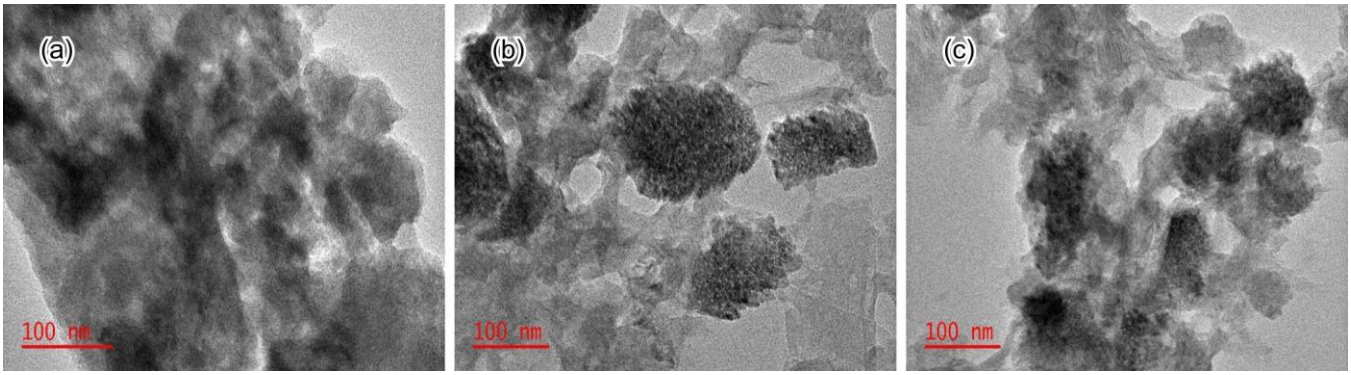

Fig. 2. TEM images of (a) CGBP, (b) AGBP, (c) BGBP adsorbents

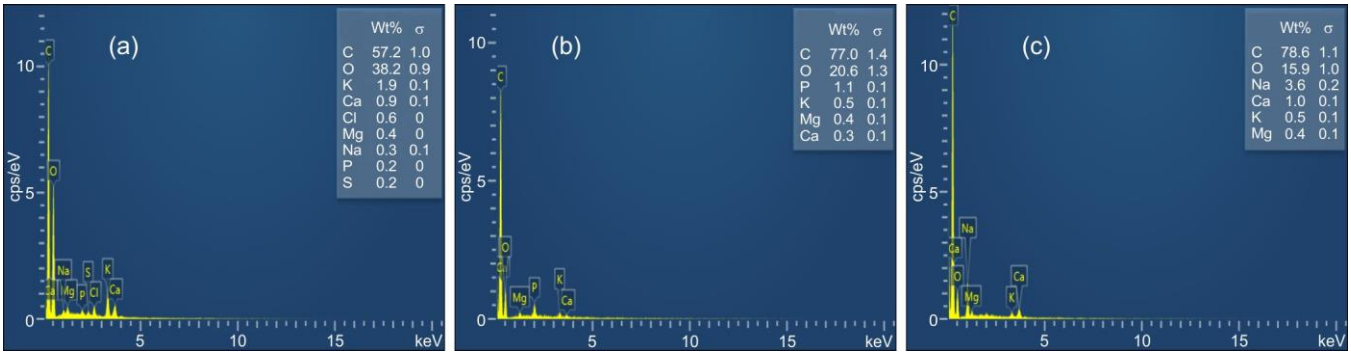

Fig. 3. EDX spectra of (a) CGBP, (b) AGBP and (c) BGBP adsorbents

horus (P) increased due to the reaction with H_3PO_4 whereas BGBP had a high content of sodium (Na) due to the reaction with NaOH [33].

FTIR studies: The FTIR spectra of untreated (CGBP), acid and base (AGBP and BGBP) activated carbons were compared to follow the changes in functional groups (Fig. 4). For CGBP, characteristic peaks for (–OH) and (–CH) were observed at around 3250 and 2916 cm^{-1}, which can be attributed to lignocellulosic and aliphatic compounds, respectively [27,34]. A peak for the aromatic ring (–C=C) and (–NH_2) moieties is assigned at 1658 cm^{-1}. The peak for the (-OH) group in cellulose was observed at 1425 cm^{-1}. The peak for the (–CO) group was recorded at 1000 cm^{-1} [35]. Changes were observed in the spectra of AGBP and BGBP after chemical activation, including the disappearance of some groups such as (–OH) at 3250 and 1435 cm^{-1} for lignocellulose and cellulose, respectively and (–CO) at 1000 cm^{-1}. In addition, the intensity of some groups such as (–CH) 2916 cm^{-1} decreased due to hydrolysis during acid and base treatment. New peaks were formed in AGBP and BGBP as highlighted in the spectra.

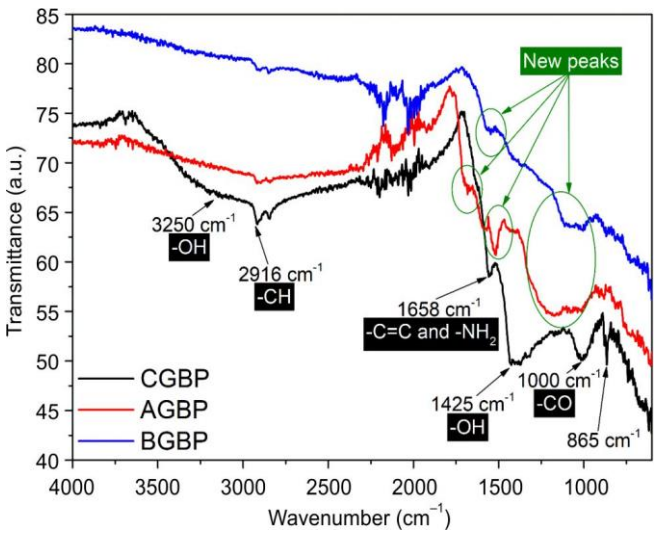

Fig. 4. FTIR spectra of CGBP, AGBP and BGBP adsorbents

XRD studies: The crystallinity was analyzed using XRD patterns (Fig. 5). The comparison shows that the samples have a broad peak between 15º and 30º, which is due to the presence of carbon [36]. The peak is indexed as [002]. BGBP only showed additional peaks around 38º and 43º, which are attributed to the graphite plane of carbon. This indicates that activation by NaOH produces carbon with a more crystalline structure than activation by H_3PO_4 (AGBP).

Raman studies: Raman spectra were used to investigate the graphitic nature of the adsorbents (Fig. 6). The samples exhibited characteristic bands attributed to the graphitic structure of carbon. The G-band was around 1606 cm^{-1} for CGBP and BGBP. However, for AGBP the band shifted slightly to 1615 cm^{-1}. The G-band confirms sp^2 hybridized orbitals in all the samples.

Adsorption studies

Temperature and initial concentration effects: The effects of initial concentration and different temperatures were investigated with standard solutions of 20, 40, 60 and 100 mg/L at the temperatures of 283, 293 and 303 K, as shown in Fig. 7a-c. Fig. 7 shows that the adsorption capacity increased when the initial concentration increased from 20 to 100 mg/L.

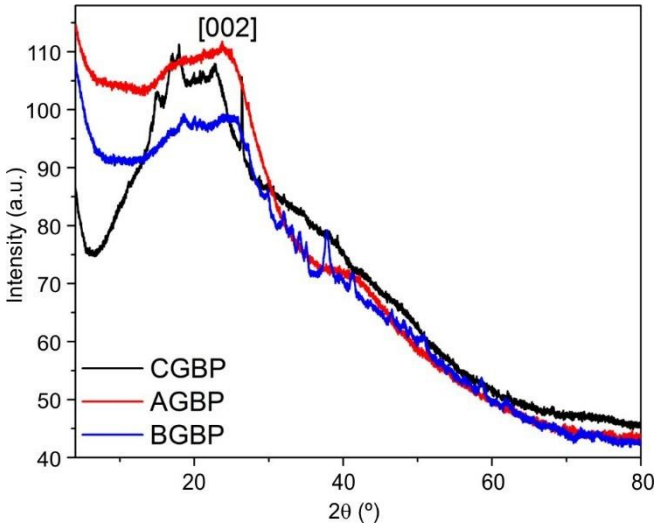

Fig. 5. XRD spectra of CGBP, AGBP and BGBP adsorbents

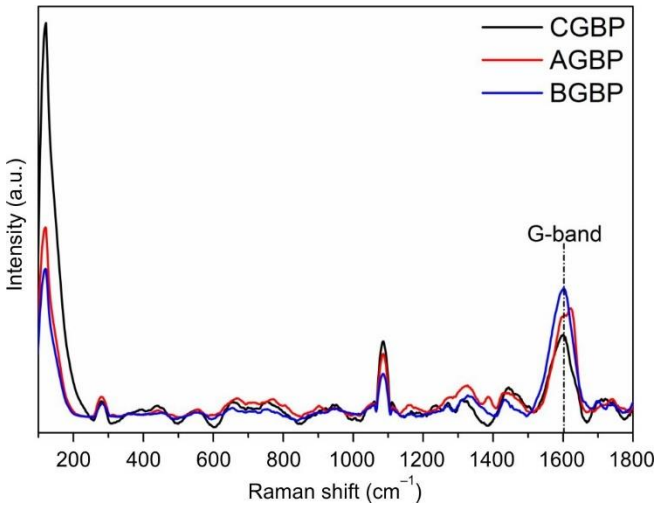

Fig. 6. Raman spectra of CGBP, AGBP and BGBP adsorbents

This enhanced mass transfer was attributed to the abundant NH_4^+ ions in the solution, which led to higher uptake [37]. The trends also show that the removal of NH_4^+ was temperature dependent. Thus, higher uptake was recorded at 283 K, but a gradual increase in temperature (293 and 303 K) had a negative effect on adsorption. At higher temperatures, the NH_4^+ ions had a higher kinetic energy, which led to increased mobility in the solution and reduced uptake [38]. The trends indicate that the adsorption is exothermic and increasing the temperature of the system had a detrimental effect on the adsorption of NH_4^+.

Thermodynamic parameters: Thermodynamic parameters (ΔH^o, ΔS^o and ΔG^o) in Table-1 were determined to verify the results obtained for the temperature effect. The values for ΔH^o and ΔG^o were negative at all temperatures, indicating that the removal of NH_4^+ by CGBP, AGBP and BGBP was exothermic and spontaneous. It shows that high temperatures did not favour the removal of NH_4^+. In general, physical adsorption occurs when the ΔH^o values are between 0 and -20 KJ/mol, while chemical adsorption occurs between -80 to -400 KJ/mol [39]. In present study, the ΔH^o values were between (-1.27 to -5.04 KJ/mol). This indicates that the uptake was controlled by physical adsorption. It was found that CGBP had the lowest values for ΔH^o in the range of -1.27 and -2.83 KJ/mol, indicating that the interaction between the adsorbent and contaminant was weak, resulting in lower adsorption [40]. On the other hand, the values for ΔH^o were higher for AGBP (-2.71 to -4.36 KJ/mol) and BGBP (-3.38 to -5.04 KJ/mol), suggesting a better interaction than for CGBP. The value of ΔS^o was also negative, indicating that the adsorption of solids and liquids at equilibrium was only partially random [41,42].

TABLE-1
THERMODYNAMIC DATA FOR THE REMOVAL OF NH_4^+

Adsorbents	Temp. (K)	Thermodynamic parameters		
		ΔH^o (KJ/mol)	ΔS^o (KJ/mol)	ΔG^o (KJ/mol)
CGBP	283	-2.831	-1.881	-6.286
	293	-1.950		
	303	-1.270		
AGBP	283	-4.362	-3.505	-12.60
	293	-3.841		
	303	-2.718		
BGBP	283	-5.041	-4.731	-14.81
	293	-4.635		
	303	-3.384		

Isotherm models: The equilibrium data using nonlinear isotherm models of Langmuir and Freundlich was used to understand the nature of the interaction during adsorption at different temperatures of 283, 293 and 303 K (Fig. 8a-c). The

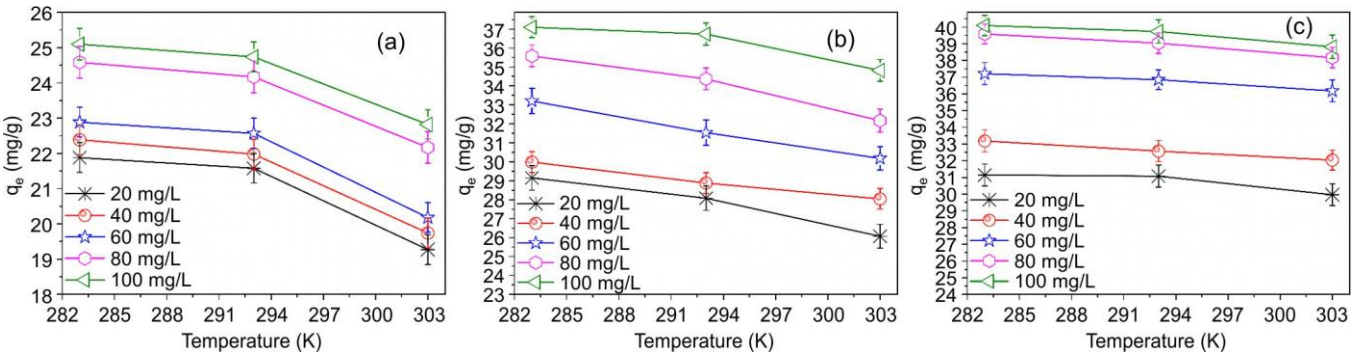

Fig. 7. Effect of initial concentration and temperature for the adsorption of NH_4^+ onto (a) CGBP, (b) AGBP and (c) BGBP [conditions: adsorbent = 100 mg, volume of NH_4^+ solution = 50 mL, agitated at 200 rpm, duration = 240 min, standard solutions used 20, 40, 60, 80 and 100 mg/L and temperature of the system 283, 293 and 303 K]

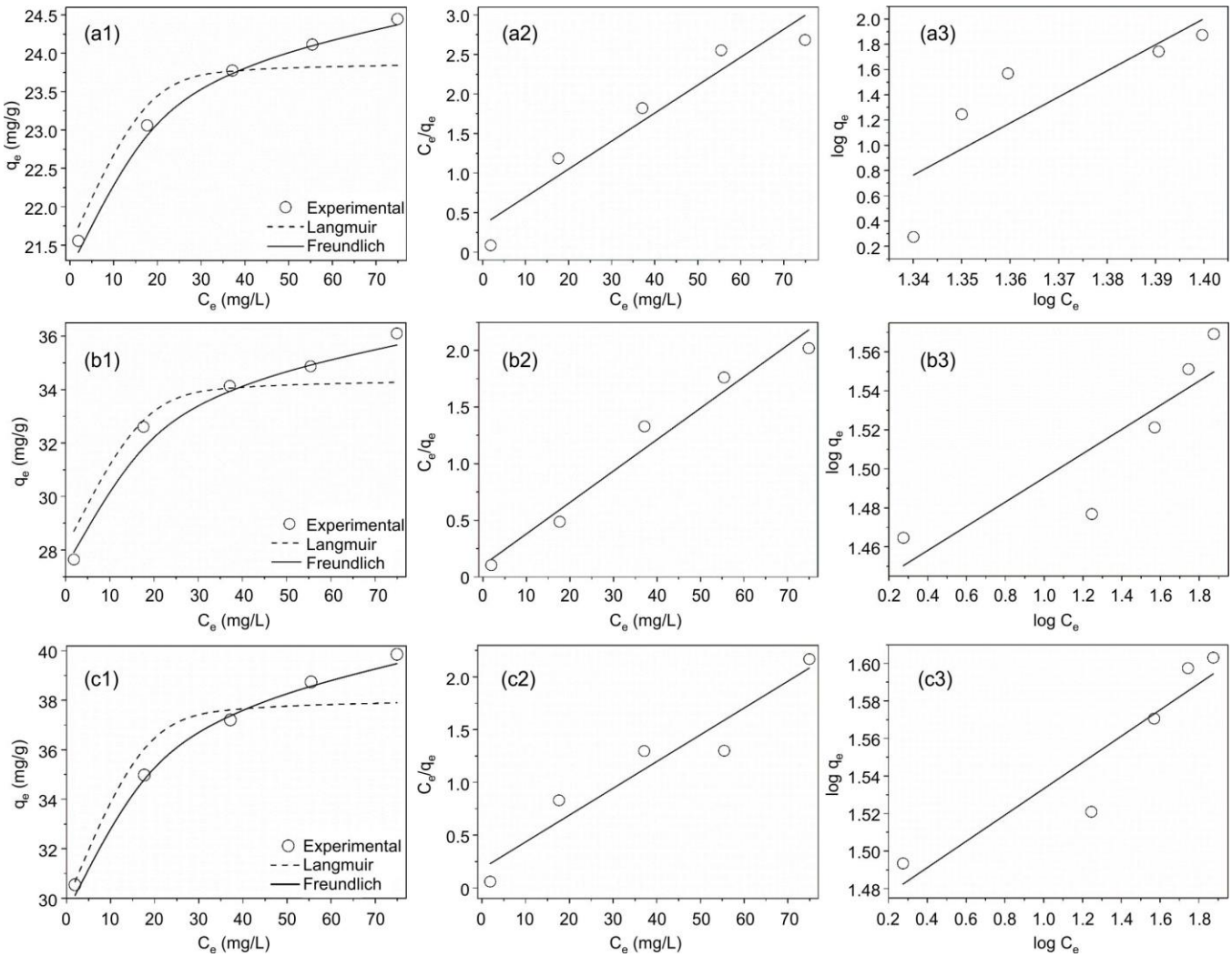

Fig. 8. Isotherm model plots of non-linear (a1,b1,c1), linear Langmuir (a2,b2,c2) and linear Freundlich (a3,b3,c3) for CGBP (a), AGBP (b) and BGBP (c) adsorbents

Langmuir model assumes the uptake of pollutants on a homogeneous surface with active sites of equal affinity, forming single-layer adsorption [43]. Freundlich, on the other hand, assumes that the adsorbent has a heterogeneous surface and can form multilayer adsorption due to different active sites with unequal energy levels [44]. The criterion for selecting a suitable model, either the Langmuir or the Freundlich isotherm, is the comparison of correlation coefficient (R^2) values that are closer to 1. The data in Table-2 show that the non-linear Freundlich isotherm has higher R^2 values than linear and non-linear Langmuir isotherms. This indicates that the data obtained fit the non-linear Freundlich model better than linear models.

TABLE-2
NONLINEAR ISOTHERMS DATA FOR THE REMOVAL OF NH_4^+

Isotherm models	Parameters	283 K			293 K			303 K		
		CGBP	AGBP	BGBP	CGBP	AGBP	BGBP	CGBP	AGBP	BGBP
Langmuir	Q_o (mg/g)	23.84	34.52	37.89	22.60	34.46	37.30	19.88	32.73	36.36
	K_L (L/mol)	0.162	0.198	0.209	0.103	0.212	0.228	0.171	0.236	0.289
	R^2	0.865	0.884	0.875	0.891	0.884	0.897	0.823	0.870	0.857
	MPSD	22.76	14.89	10.42	14.25	8.649	7.530	12.69	11.74	9.217
Freundlich	q_e	24.37	35.67	39.48	24.69	36.61	39.74	22.68	34.80	38.91
	K_F	1.992	2.813	2.943	1.892	2.887	2.901	1.905	2.735	2.863
	N	4.276	5.580	5.902	3.053	4.211	5.132	2.314	2.937	3.408
	R^2	0.995	0.997	0.995	0.996	0.998	0.997	0.995	0.998	0.998
	MPSD	4.781	2.594	2.648	6.305	2.025	5.401	5.744	3.952	1.023
Experimental	q_e (mg/g)	25.09	37.04	40.11	24.74	36.69	39.81	22.77	34.82	38.95

The model also predicted adsorption capacities (q_e) that were closer to the experimental values (q_e). At 283, 293 and 303 K the non-linear Freundlich constant (K_F) was higher for AGBP and BGBP, indicating that the materials had a higher affinity for NH_4^+ than CGBP. In general, the Freundlich constant (n) for favourable uptake should be between 0 and 10 [45]. The Marquart percentage standard deviation (MPSD) was used to validate the isotherm models, with lower MPSD values indicating a more suitable model, and the non-linear Freundlich model was found to have lower MPSD values than the Langmuir model. This confirms that the adsorption data fits the non-linear Freundlich model better.

Effect of pH: The pH value of the solution is of crucial importance in adsorption processes, as it influences the surface charge of the adsorbent and changes the speciation of the pollutant. The effect of solution pH was analysed for NH_4^+ between pH 2-10 and the results are shown in Fig. 9. The trends show that uptake increased when the pH of the solution was increased, with pH 10 being the optimum. At acidic conditions between pH 2-6, uptake was lowest, probably due to the protonation of the adsorbent and the presence of H^+. The functional groups acquired a positive charge and the speciation of the contaminant was NH_4^+ [46]. This limited the interaction between the positively charged adsorbent and the NH_4^+ ions. These conditions resulted in enhanced repulsive forces and minimization of the electrostatic interaction, leading to other mechanisms controlling the uptake. In contrast, under alkaline conditions between pH 8-10, the pollutant is present as a neutral NH_3 molecule and the adsorbent was deprotonated and acquired a negative charge [47]. NH_3, which has a lone pair of electrons, may have interacted with the deprotonated surface of the adsorbent by sharing the lone electrons and forming bonds. The maximum uptake occurred at pH 10.

Effect of contact time: The rate of NH_4^+ uptake by the adsorbents until equilibrium was reached was evaluated at 283, 293 and 303 K and the trends are shown in Fig. 10a-c. At 283 K (Fig. 10a) the trend for CGBP showed three distinct phases of adsorption. Phase one showed a sharp increase (in the first 30 min) due to the availability of numerous adsorption sites. Phase two showed steady adsorption (between 30-60 min), which is attributed to a slower diffusion process of the NH_4^+ molecules from the outer to the inner surface through the pores, voids and openings. In phase three, a plateau was recorded (between 60-240 min), indicating a saturation point and the

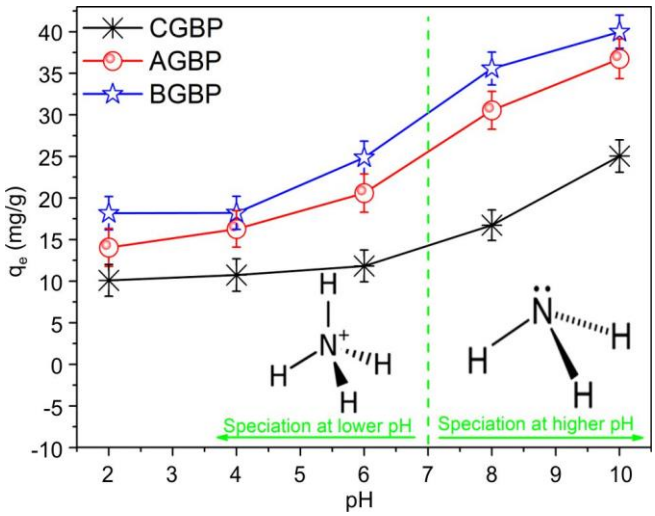

Fig. 9. Effect of pH for the adsorption of NH_4^+ species [conditions: adsorbent = 100 mg, volume of NH_4^+ solution = 50 mL, agitated at 200 rpm, duration = 240 min, standard solution used 100 mg/L and temperature of the system 283 K]

achievement of equilibrium. On the other hand, at higher temperatures 298 and 303 K (Fig. 10b-c), the trends showed two distinct phases only: a sharp increase at the beginning stages and a plateau. At temperatures 293 and 303 K, the values for the experimental q_e progressively decreased due to the exothermic nature slowing down the adsorption of NH_4^+.

Kinetic studies: The contact time data were fitted at 283, 293 and 303 K to pseudo-first-order (PFO) and pseudo-second-order (PSO) kinetic models to determine the model that best fits the data (Table-3). The PFO assumes that the uptake of pollutants occurs by physical adsorption, determined by weak van der Waals forces [48]. The PSO assumes that uptake occurs through a chemical process in which electrons are shared or transferred between the adsorbent and contaminant, resulting in various interactions such as electrostatic, hydrogen bonding [49]. As a criterion for selecting an appropriate model, we compared correlation coefficient (R^2) values closer to 1. The PSO had values closer to 1 compared to the PFO. This suggests that the uptake of NH_4^+ by CGBP, AGBP and BGBP follows the PSO. This model also predicted adsorption capacities closer to the experimental q_e. At 283 K the values of the PSO constant (K_2) range between ($3.872 \times 10^{-3} - 4.690 \times 10^{-3}$), indicating that the uptake is fast. Therefore, the equilibrium for AGBP

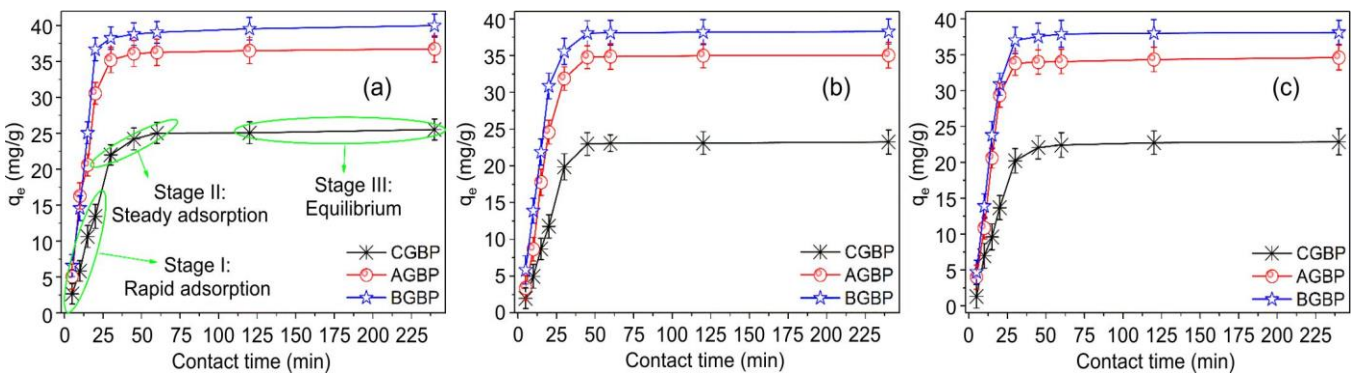

Fig. 10. Effect of contact time for the adsorption of NH_4^+ at (a) 283 K, (b) 293 K and (c) 303 K [Adsorption conditions: adsorbent = 100 mg, volume of NH_4^+ solution = 50 mL, agitated at 200 rpm, duration = 5-240 min, standard solutions used 100 mg/L and temperature of the system 283, 293 and 303 K]

TABLE-3
KINETIC DATA FOR THE REMOVAL OF NH_4^+

Kinetics models	Parameters	Adsorbents		
		CGBP	AGBP	BGBP
PFO	q_e (mg/g)	16.33	25.16	30.72
	K_1 (min^{-1})	0.063	0.081	0.085
	R^2	0.725	0.771	0.736
PSO	q_e (mg/g)	25.31	37.22	40.07
	K_2 (g mg/min) × 10^{-3}	3.872	4.538	4.690
	R^2	0.999	0.999	0.999
Experimental	q_e (mg/g)	25.09	37.04	40.11

and BGBP was reached within 40 min while for CGBP it took 60 min.

Post-adsorption studies

SEM: The surface of CGBP after adsorption was analysed by SEM and the images are shown in Fig 11a-b. A change in the surface morphology was observed with the formation of spherical particles which were not present in Fig. 1a-f. It is assumed that this is due to the adsorption of NH_4^+ on the surface of the material.

FTIR: The FTIR spectra of CGBP before and after adsorption were compared to observe the changes that occurred during the uptake of NH_4^+ (Fig. 12). Before adsorption, CGBP was found to have several moieties, such as –OH (3250 cm^{-1}), –CH (2916 cm^{-1}), –C=C and $–NH_2$ groups (1658 cm^{-1}), –OH (1425 cm^{-1}), –CO (1000 cm^{-1}) and a peak at 865 cm^{-1}. After adsorption, the positions of some moieties shifted slightly as follows: –OH (3257 cm^{-1}), –CH (2920 cm^{-1}) and –CO (1048 cm^{-1}). Some components retained their positions, but the intensity of the peaks decreased significantly after adsorption: –C=C and $–NH_2$ groups (1658 cm^{-1}), –OH (1425 cm^{-1}) and

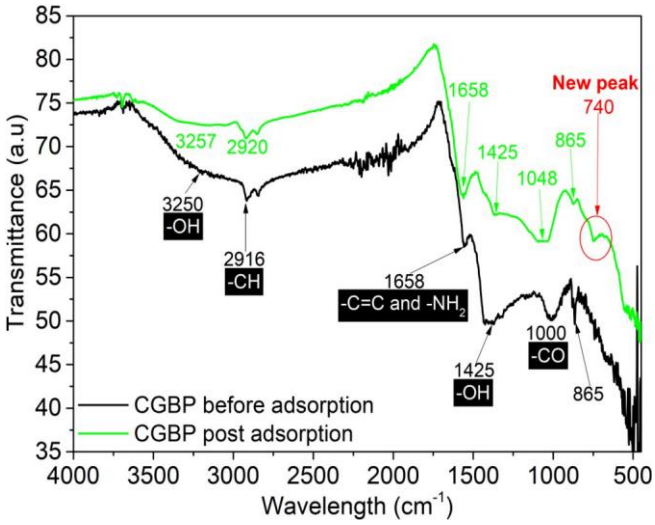

Fig. 12. FTIR spectra for CGBP before and after adsorption

peak at 865 cm^{-1}. These changes and variables demonstrate the synergistic involvement of different moieties in the uptake of NH_4^+. After adsorption, a new peak at 740 cm^{-1} was observed. Similar results were reported when carbon from peanut shells used [50].

Mechanism: The proposed adsorption mechanism (**Scheme-I**) was established based on the results in Fig. 10, isotherms, kinetics and thermodynamic studies. The ΔH^o values were between (-1.27 to -5.04 KJ/mol). This indicates that the uptake was dominated by physical adsorption. But to some extent other mechanisms were partially involved in the uptake. After adsorption, the FTIR studies showed that numerous components on the surface of the material were involved in the uptake. The moieties such as –OH (hydroxyl) and –NH

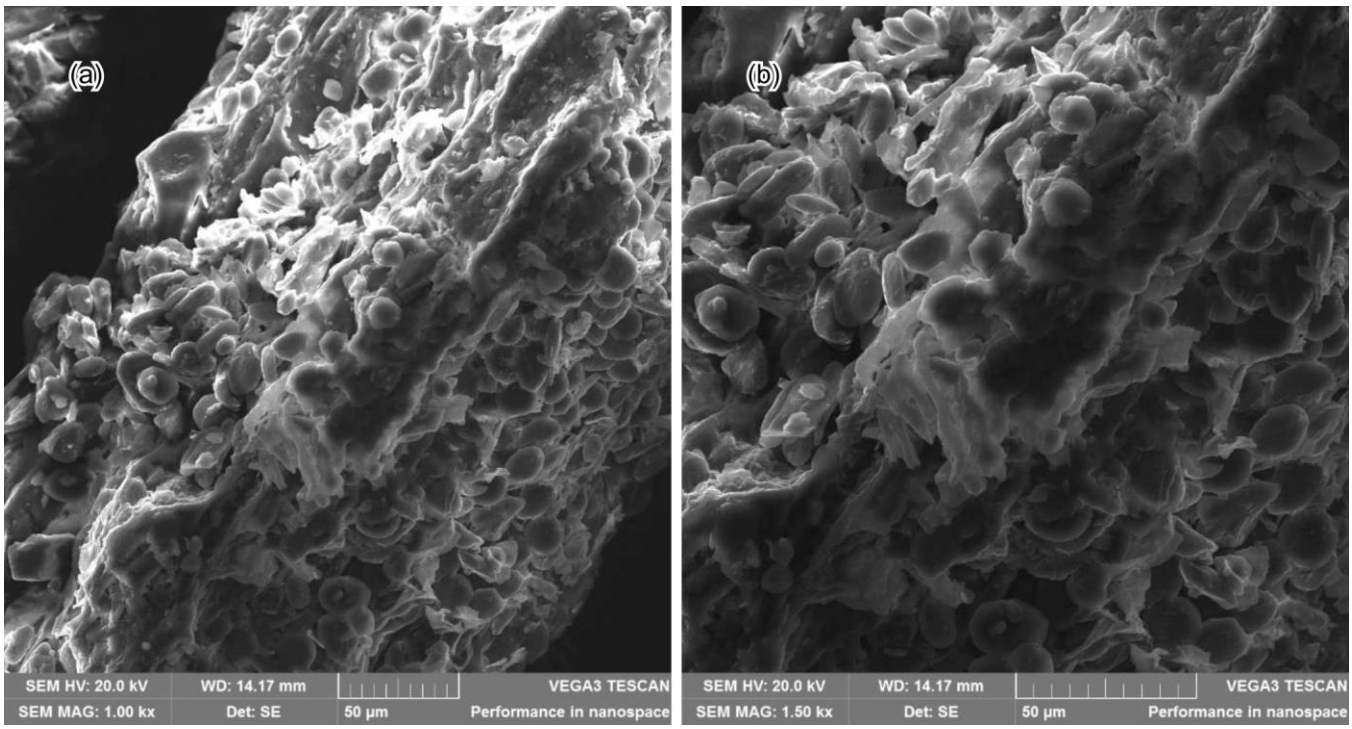

Fig. 11. SEM images (a-b) for CGBP after adsorption

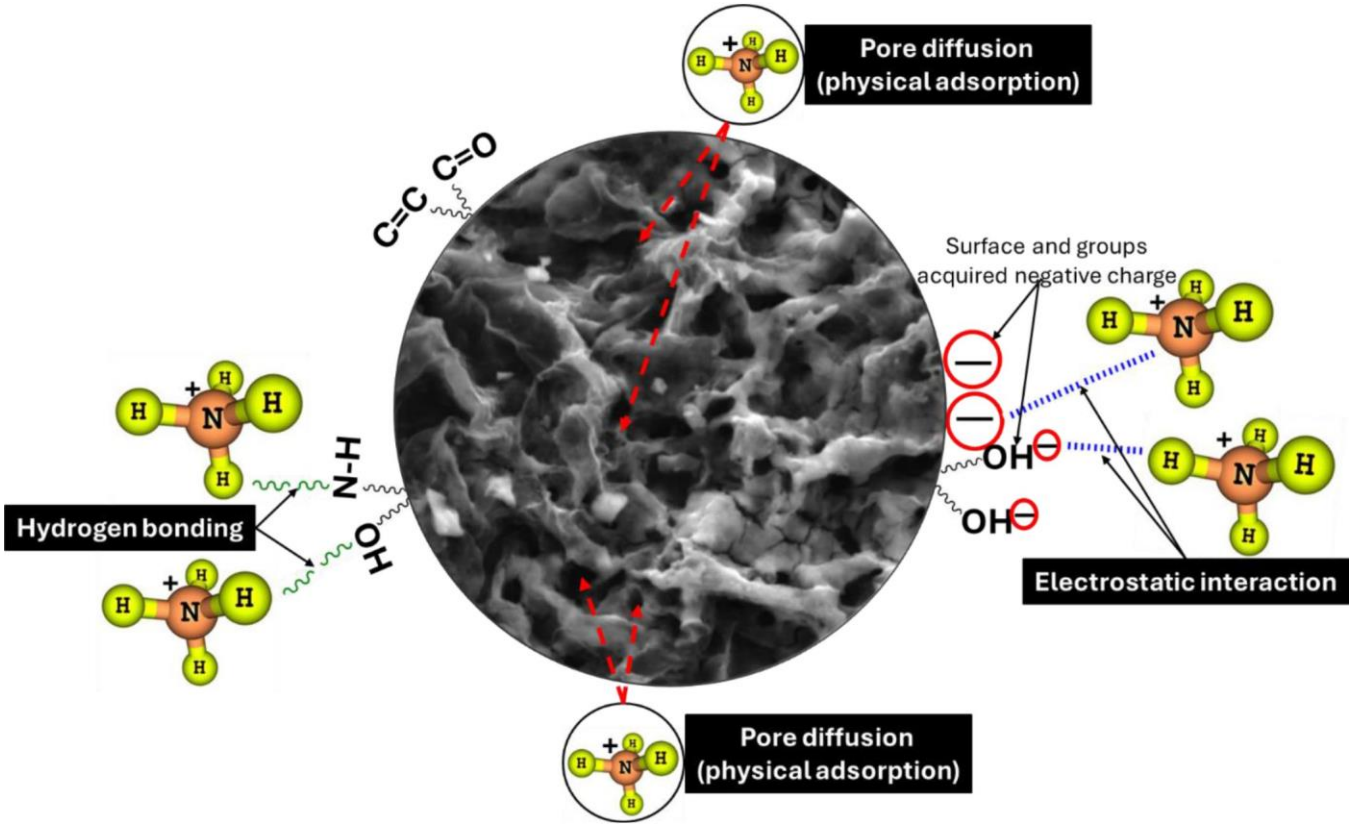

Scheme-I: Proposed adsorption mechanism for the removal of NH_4^+ onto activated carbon produced from garlic basal plate waste

(amine) interacted with NH_4^+ to form hydrogen bonds. Under alkaline conditions, the surface of the material was deprotonated and acquired a negative charge, leading to an electrostatic interaction with NH_4^+. The data obtained were consistent with the Freundlich model, indicating that multilayer adsorption had formed.

Comparative studies: The best-performing adsorbent in this study was BGBP with a maximum adsorption capacity of 40.11 mg/g. This result was compared with similar carbon-based materials as shown in Table-4. BGBP exhibited a higher adsorption capacity than other carbon-based materials, attributed to enhanced properties such as porous structure and abundant surface active sites, indicating its strong potential for water treatment applications.

Reusability and regeneration: The applicability of garlic waste as an adsorbent for water treatment was tested by investigating its reusability and regeneration (Fig. 13). A 0.5 M HCl solution was used for regeneration and the spent adsorbent was soaked after each use of the material to desorb the NH_4^+ ions. The reusability trends over cycles 1-4 showed that adsorption uptake increased in the first cycle and then gradually decreased in the subsequent cycles. The uptake of AGBP and BGBP was still reliable after four cycles, with an efficiency of more than 70%.

TABLE-4
COMPARATIVE DATA OF THE REMOVAL OF NH_4^+ USING DIFFERENT CARBON-BASED MATERIALS

Biosorbent	Activation agent	q_e (mg/g)	Ref.
Activated carbon	Sodium dodecyl sulfate	1.700	[51]
Biochar from sawdust	–	2.201	[52]
Activated carbon from coconut shell	H_3PO_4	2.300	[53]
Carbon from coffee husk	–	2.800	[54]
Activated carbon from corncob	NaOH	2.900	[55]
Biochar from *phragmites communis*	–	3.206	[52]
Biochar from fruit pericarp	–	3.250	[56]
Biochar from rice straw	–	4.090	[52]
Activated carbon from papaya peel	KOH	4.600	[57]
Biochar from orange peel	–	4.710	[58]
Activated biochar from banana leaves	NaOH	5.150	[44]
Biochar from sesame straw	–	26.84	[59]
Biochar from spent coffee grounds	KOH	51.52	[60]
Activated carbon from garlic waste	NaOH	40.11	Present study

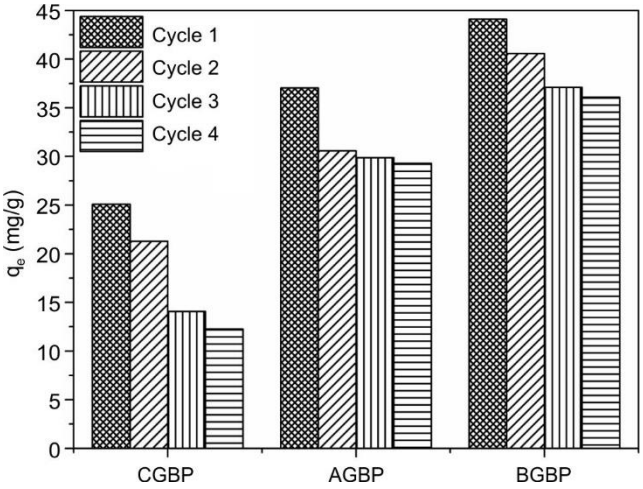

Fig. 13. Reusability data for CGBP, AGBP and BGBP towards NH_4^+

Conclusion

This research investigated the successful removal of NH_4^+ from water by activated carbon derived from garlic basal plate waste. After activation, it was found that the inner surface was exposed. The surface is heterogeneous, porous and has cavities of different shapes and sizes. The elemental components of the materials are carbon (C), oxygen (O) and heteroatoms in traces amounts. FTIR analysis showed that the materials contained several groups such as –OH (3250 cm^{-1}), –CH (2916 cm^{-1}), –C=C and $–NH_2$ (1658 cm^{-1}), –OH (1425 cm^{-1}) and –CO (1000 cm^{-1}). The adsorption results for the temperature effect showed that the uptake was temperature dependent. Thus, a higher uptake was recorded at 283 K, but a gradual increase in temperature (293 and 303 K) affected adsorption negatively. The ΔH^o values ranged from (-1.27 to -5.04 KJ/mol), indicating that the uptake was dominated by physical adsorption, but to some extent other mechanisms were partially involved in the uptake. The values of ΔS^o and ΔG^o were also negative, denoting that the adsorption was spontaneous and that the adsorption of solids and liquids at equilibrium was only partially random. The obtained data corresponds to the non-linear Freundlich model which assumes that the uptake forms multilayer adsorption due to different active sites on the adsorbent with unequal energy levels. The Freundlich constant (*n*) gave values between 4.276 and 5.902, indicating that the uptake was favourable. The effect of pH showed that uptake increased as the pH of the solution was increased, with pH 10 being the optimum. Contact time studies showed that uptake exhibited three distinct phases of adsorption. Phase one showed a sharp increase, phase two a steady adsorption and phase three a plateau. The reusability of the adsorbents showed that the uptake by AGBP and BGBP was still good after four cycles with an efficiency of more than 70%. These results show the potential and feasibility of garlic waste in water treatment. Further research should include investigating different carbonization techniques for garlic basal plate waste such as the use of a microwave and hydrothermal energy. The activation of carbon with stronger oxidation agents such as HNO_3, H_2SO_4 and H_2O_2 is recommended. This activated carbon could be used for the adsorption of other emerging pollutant, dyes and metal ions.

CONFLICT OF INTEREST

The authors declare that there is no conflict of interests regarding the publication of this article.

DECLARATION OF AI-ASSISTED TECHNOLOGIES

The authors declare that no AI tools were used in the preparation or writing of this research/review article.

REFERENCES

1. R.R. Karri, J.N. Sahu and V. Chimmiri, *J. Mol. Liq.*, **261**, 21 (2018); https://doi.org/10.1016/j.molliq.2018.03.120
2. A. Omar, F. Almomani, H. Qiblawey and K. Rasool, *Sustainability*, **16**, 2112 (2024); https://doi.org/10.3390/su16052112
3. J. Huang, N.R. Kankanamge, C. Chow, D.T. Welsh, T. Li and P.R. Teasdale, *J. Environ. Sci. (China)*, **63**, 174 (2018); https://doi.org/10.1016/j.jes.2017.09.009
4. H.W. Paerl, T.G. Otten and R. Kudela, *Environ. Sci. Technol.*, **52**, 5519 (2018); https://doi.org/10.1021/acs.est.7b05950
5. World Health Organization, Guidelines for Drinking-Water Quality, 2nd ed., vol. 2: Health Criteria and Other Supporting Information. Geneva: World Health Organization (1996).
6. J. Lan, P. Liu, X. Hu and S. Zhu, *Water*, **16**, 2525 (2024); https://doi.org/10.3390/w16172525
7. S. Dasarathy, R.P. Mookerjee, V. Rackayova, V. Rangroo Thrane, B. Vairappan, P. Ott and C.F. Rose, *Metab. Brain Dis.*, **32**, 529 (2017); https://doi.org/10.1007/s11011-016-9938-3
8. X. Zeng, R. Liu, Y. Li, J. Li, Q. Zhao, X. Li and J. Bao, *Ecotoxicol. Environ. Saf.*, **217**, 112203 (2021); https://doi.org/10.1016/j.ecoenv.2021.112203
9. P.M. Thabede, N.D. Shooto and E.B. Naidoo, *Asian J. Chem.*, **33**, 471 (2021); https://doi.org/10.14233/ajchem.2021.23021
10. P.M. Thabede, N.D. Shooto, T. Xaba and E.B. Naidoo, *Asian J. Chem.*, **32**, 1361 (2020); https://doi.org/10.14233/ajchem.2020.22597
11. B.R. Mphuthi, P.M. Thabede, M.E. Monapathi and N.D. Shooto, *Case Stud. Chem. Environ. Eng.*, **8**, 100436 (2023); https://doi.org/10.1016/j.cscee.2023.100436
12. R.S. Riseh, M.G. Vazvani, M. Hassanisaadi and V.K. Thakur, *Ind. Crops Prod.*, **208**, 117904 (2024); https://doi.org/10.1016/j.indcrop.2023.117904
13. N. Mabungela, N.D. Shooto, E.D. Dikio, S.J. Modise, M.E. Monapathi, F.M. Mtunzi, T. Xaba and E.B. Naidoo, *Environ. Chem. Ecotoxicol.*, **4**, 171 (2022); https://doi.org/10.1016/j.enceco.2022.09.001
14. N.D. Shooto and E.B. Naidoo, *Asian J. Chem.*, **31**, 2249 (2019); https://doi.org/10.14233/ajchem.2019.22051
15. N.D. Shooto, *Desalination Water Treat.*, **320**, 100812 (2024); https://doi.org/10.1016/j.dwt.2024.100812
16. J. Ansary, T.Y. Forbes-Hernandez, E. Gil, D. Cianciosi, J. Zhang, M. Elexpuru-Zabaleta, J. Simal-Gandara, F. Giampieri and M. Battino, *Antioxidants*, **9**, 619 (2020); https://doi.org/10.3390/antiox9070619
17. A.M. Aljeboree, A.Y. Al-Baitai, S.M. Abdalhadi and A.F. Alkaim, *Egypt. J. Chem.*, **64**, 2873 (2021); https://doi.org/10.21608/ejchem.2021.55274.3159
18. A.M. Aljeboree, A.F. Alkaim and A.H. Al-Dujaili, *Desalination Water Treat.*, **53**, 3656 (2015); https://doi.org/10.1080/19443994.2013.877854
19. A.M. Aljeboree, A.N. Alshirifi and A.F. Alkaim, *Arab. J. Chem.*, **10**, 3381 (2017); https://doi.org/10.1016/j.arabjc.2014.01.020
20. S. Liang, X. Guo and Q. Tian, *Desalination Water Treat.*, **51**, 7166 (2013); https://doi.org/10.1080/19443994.2013.769919

21. M.S. Abu-Shahba, M.M. Mansour, H.I. Mohamed and M.R. Sofy, *Sci. Hortic.*, **293**, 110727 (2022); https://doi.org/10.1016/j.scienta.2021.110727
22. Z.M. Saigl and E.E. Aloufi, *Desalination Water Treat.*, **294**, 149 (2023); https://doi.org/10.5004/dwt.2023.29569
23. Q. Chang, P. Li, Y. Han, X. Guan, J. Xiong, Q. Li, H. Zhang, K. Huang, X. Zhang, H. Xie and T. Qi, *J. Environ. Chem. Eng.*, **11**, 109997 (2023); https://doi.org/10.1016/j.jece.2023.109997
24. P. Muthamilselvi, R. Karthikeyan and B.S.M. Kumar, *Desalination Water Treat.*, **57**, 2089 (2016); https://doi.org/10.1080/19443994.2014.979237
25. B.H. Hameed and A.A. Ahmad, *J. Hazard. Mater.*, **164**, 870 (2009); https://doi.org/10.1016/j.jhazmat.2008.08.084
26. M.F. Elshahawy, N.A. Ahmed and G.A. Mahmoud, *Mater. Chem. Phys.*, **321**, 129487 (2024); https://doi.org/10.1016/j.matchemphys.2024.129487
27. D. Pathania, V.S. Bhat, J. Mannekote Shivanna, G. Sriram, M. Kurkuri and G. Hegde, *Spectrochim. Acta A Mol. Biomol. Spectrosc.*, **276**, 121197 (2022); https://doi.org/10.1016/j.saa.2022.121197
28. Y. Zhao, L. Zhu, W. Li, J. Liu, X. Liu and K. Huang, *J. Mol. Liq.*, **293**, 111516 (2019); https://doi.org/10.1016/j.molliq.2019.111516
29. Y. Zhao, X. Liu, W. Li, K. Huang, H. Shao, C. Qu and J. Liu, *Chemosphere*, **290**, 133263 (2022); https://doi.org/10.1016/j.chemosphere.2021.133263
30. Y. Omidi-Khaniabadi, A. Jafari, H. Nourmoradi, F. Taheri and S. Saeedi, *J. Adv. Environ. Health Res.*, **3**, 120 (2015).
31. N.D. Shooto and P.M. Thabede, *Chem. Thermodyn. Therm. Anal.*, **20**, 100237 (2025); https://doi.org/10.1016/j.ctta.2025.100237
32. N.D. Shooto and P.M. Thabede, *Desalination Water Treat.*, **324**, 101543 (2025); https://doi.org/10.1016/j.dwt.2025.101543
33. Y. Li, X. Zhang, R. Yang, G. Li and C. Hu, *RSC Adv.*, **5**, 32626 (2015); https://doi.org/10.1039/C5RA04634C
34. J. Zhuang, M. Li, Y. Pu, A.J. Ragauskas and C.G. Yoo, *Appl. Sci.*, **10**, 4345 (2020); https://doi.org/10.3390/app10124345
35. T.T. Shi, B. Yang, W.G. Hu, G.J. Gao, X.Y. Jiang and J.G. Yu, *Molecules*, **29**, 4772 (2024); https://doi.org/10.3390/molecules29194772
36. S. Adhikari, E. Moon, J. Paz-Ferreiro and W. Timms, *Sci. Total Environ.*, **914**, 169607 (2024); https://doi.org/10.1016/j.scitotenv.2023.169607
37. N.D. Shooto, *Heliyon*, **9**, 20268 (2023); https://doi.org/10.1016/j.heliyon.2023.e20268
38. K. Zhu, H. Fu, J. Zhang, X. Lv, J. Tang and X. Xu, *Biomass Bioenergy*, **43**, 18 (2012); https://doi.org/10.1016/j.biombioe.2012.04.005
39. P.D. Humpola, H.S. Odetti, A.E. Fertitta and J.L. Vicente, *J. Chil. Chem. Soc.*, **58**, 1541 (2013); https://doi.org/10.4067/S0717-97072013000100009
40. E.M. Abdel-Hamid, H.M. Aly and K.A.M. El-Naggar, *Sci. Rep.*, **14**, 20631 (2024); https://doi.org/10.1038/s41598-024-70284-y
41. K. Mabalane, N.D. Shooto and P.M. Thabede, *Case Studies in Chemical and Environmental Engineering*, **10**, 100782 (2024a); https://doi.org/10.1016/j.cscee.2024.100782
42. N. Nkosi, N.D. Shooto, P. Nyamukamba and P.M. Thabede, *Energy Nexus*, **15**, 100313 (2024); https://doi.org/10.1016/j.nexus.2024.100313
43. A. Khamkeaw, W. Sanprom and M. Phisalaphong, *Case Stud. Chem. Environ. Eng.*, **8**, 100499 (2023); https://doi.org/10.1016/j.cscee.2023.100499
44. F. Pantoja, S. Beszedes, T. Gyulavari, E. Illes, G. Kozma and Z. Laszlo, *Heliyon*, **10**, 31495 (2024); https://doi.org/10.1016/j.heliyon.2024.e31495
45. K. Mabalane, P.M. Thabede and N.D. Shooto, *Green Anal. Chem.*, **10**, 100135 (2024); https://doi.org/10.1016/j.greeac.2024.100135
46. S. Nezami, A. Ghaemi and T. Yousefi, *Case Stud. Chem. Environ. Eng.*, **7**, 100326 (2023); https://doi.org/10.1016/j.cscee.2023.100326
47. A.H. Ragab, A.M. Zayed, B.S. Metwally, N.F. Gumaah, M.F. Mubarak, H. Shendy, A.M. Abd-Elgawad, M.M. Abdelsatar, M.S.M. Abdel Wahed and M.A. Masoud, *Desalination Water Treat.*, **320**, 100809 (2024); https://doi.org/10.1016/j.dwt.2024.100809
48. T.A. Saleh, *Interface Sci. Technol.*, **34**, 39 (2022); https://doi.org/10.1016/B978-0-12-849876-7.00006-3
49. M.O. Omorogie and B. Helmreich, *Ind. Eng. Chem. Res.*, **63**, 3947 (2024); https://doi.org/10.1021/acs.iecr.3c03971
50. Z. Wang, J. Li, G. Zhang, Y. Zhi, D. Yang, X. Lai and T. Ren, *Materials*, **13**, 2270 (2020); https://doi.org/10.3390/ma13102270
51. W. Lee, S. Yoon, J.K. Choe, M. Lee and Y. Choi, *Sci. Total Environ.*, **639**, 1432 (2018); https://doi.org/10.1016/j.scitotenv.2018.05.250
52. D. Xu, J. Cao, Y. Li, A. Howard and K. Yu, *Waste Manag.*, **87**, 652 (2019); https://doi.org/10.1016/j.wasman.2019.02.049
53. R. Boopathy, S. Karthikeyan, A.B. Mandal and G. Sekaran, *Environ. Sci. Pollut. Res. Int.*, **20**, 533 (2013); https://doi.org/10.1007/s11356-012-0911-3
54. N.T. Vu and K.U. Do, *Biomass Convers. Biorefin.*, **13**, 2193 (2023); https://doi.org/10.1007/s13399-021-01337-9
55. M.T. Vu, H.P. Chao, T. Van Trinh, T.T. Le, C.C. Lin and H.N. Tran, *J. Clean. Prod.*, **180**, 560 (2018); https://doi.org/10.1016/j.jclepro.2018.01.104
56. S. Xue, X. Zhang, H.H. Ngo, W. Guo, H. Wen, C. Li, Y. Zhang and C. Ma, *Bioresour. Technol.*, **292**, 121927 (2019); https://doi.org/10.1016/j.biortech.2019.121927
57. A. Musa, S.R.W. Alwi, N. Ngadi and S. Abbaszadeh, *Chem. Eng. Trans.*, **56**, 841 (2017); https://doi.org/10.3303/CET1756141
58. H. Hu, X. Zhang, H.H. Ngo, W. Guo, H. Wen, C. Li, Y. Zhang and C. Ma, *Sci. Total Environ.*, **707**, 135544 (2020); https://doi.org/10.1016/j.scitotenv.2019.135544
59. Q. Yin, B. Zhang, R. Wang and Z. Zhao, *Environ. Sci. Pollut. Res. Int.*, **25**, 4320 (2018); https://doi.org/10.1007/s11356-017-0778-4
60. V.T. Nguyen, T.D.H. Vo, T. Tran, T.N. Nguyen, T.N.C. Le, X.T. Bui and L.G. Bach, *Case Case Stud. Chem. Environ. Eng.*, **4**, 100141 (2021); https://doi.org/10.1016/j.cscee.2021.100141